

# Exploring the morphology of adult tibia and fibula from Sima de los Huesos site in sierra de Atapuerca, Burgos, Spain

Laura Rodríguez<sup>1,2</sup>  | Rebeca García-González<sup>2</sup>  | Juan Luis Arsuaga<sup>3,4</sup>  | José-Miguel Carretero<sup>2,4,5</sup> 

<sup>1</sup>Area de Antropología Física. Departamento de Biodiversidad y Gestión Ambiental, Universidad de León. Facultad de Ciencias Biológicas y Ambientales. Campus De Vegazana, León, España

<sup>2</sup>Laboratorio de Evolución Humana, Universidad de Burgos, Burgos, España

<sup>3</sup>Departamento de Geodinámica, Estratigrafía y Paleontología, Facultad de Ciencias Geológicas, Universidad Complutense de Madrid, Madrid, Spain

<sup>4</sup>Centro UCM-ISCIH de Investigación sobre Evolución y Comportamiento Humanos, Madrid, Spain

<sup>5</sup>Unidad Asociada de I+D+i al CSIC Vidrio y Materiales del Patrimonio Cultural (VIMPAC), Universidad de Burgos, Burgos, España

## Correspondence

Laura Rodríguez, Departamento de Biodiversidad y Gestión Ambiental, Universidad de León. Facultad de Ciencias Biológicas y Ambientales. Campus De Vegazana. Avda. Emilio Hurtado s/n 24071 León, Spain.  
Email: [lrodg@unileon.es](mailto:lrodg@unileon.es)

## Funding information

MCIN/AEI/10.13039/501100011033/  
FEDER, UE grant number PID2021-  
122355NB-C31

## Abstract

The analysis of the locomotor anatomy of Late Pleistocene *Homo* has largely focused on changes in proximal femur and pelvic morphologies, with much attention centered on the emergence of modern humans. Although much of the focus has been on changes in the proximal femur, some research has also been conducted on tibiae and, to a lesser extent, fibulae. With this in mind, we present one of the largest samples of the same population of human tibiae and fibulae from the Middle Pleistocene to determine their main characteristic traits and establish similarities and differences, primarily with those of Neanderthals and modern humans, but also with other Middle Pleistocene specimens in the fossil record. Through this study, we established that the Middle Pleistocene population from the Sima de los Huesos (Atapuerca, Burgos, Spain) had lower leg long bones similar to those of Neanderthals, although there were some important differences, such as bone length, which this fossil individuals resembled those of modern humans and not to Neanderthals. This fact is related to the crural index and leg length, even though we do not have any true association between femora and tibiae yet, it has implications for establishing locomotor efficiency and climate adaptation.

## KEYWORDS

activity, fibula, Sima de los Huesos, tibia

This is an open access article under the terms of the [Creative Commons Attribution-NonCommercial-NoDerivs](https://creativecommons.org/licenses/by-nc-nd/4.0/) License, which permits use and distribution in any medium, provided the original work is properly cited, the use is non-commercial and no modifications or adaptations are made.

© 2023 The Authors. *The Anatomical Record* published by Wiley Periodicals LLC on behalf of American Association for Anatomy.

## 1 | INTRODUCTION

Complete tibia and fibula remains are relatively scarce in the fossil human record, but they can be extremely important in shedding light on locomotion and weight transmission (Marchi & Shaw, 2011; Squyres & Ruff, 2015). And although much attention has focused on changes in pelvic and femoral morphology and their implications (e.g., Arsuaga et al., 1999; Bonmatí et al., 2010; Rosenberg et al., 2006; Ruff et al., 1993; Simpson et al., 2008), only some of them are based on tibiae analysis and importance (and only for some examples, Aiello & Dean, 1990; Lockey et al., 2022; Marchi, 2007; Roberts et al., 1994; Ruff & Hayes, 1988; Stringer et al., 1998; Shaw & Stock, 2009; Trinkaus, 2009) and to the fossil fibulae (Aiello & Dean, 1990; Marchi, 2007, 2015; Marchi et al., 2017; Marchi & Shaw, 2011; Sparacello et al., 2014). Thus, one of our aims here is to present one of the biggest samples of tibiae and fibulae from the European Middle Pleistocene and determine their main morphological traits.

The appearance of Neanderthal morphology in the postcranial fossil record is shown to have occurred during the Middle Pleistocene in Europe (Arsuaga et al., 2014, 2015), but also in some Middle Pleistocene specimens in Africa, as seen in the Berg Aukas femur or Bodo humerus (Carretero et al., 2009; Grine et al., 1995; Trinkaus et al., 1999) but not in others as Broken Hill tibia (Trinkaus, 2009).

Primitive traits recorded in Neanderthal tibiae are a sloped tibial plateau, projected tibial tuberosity and posterior condyle location, and plactynemia. Until now, most of the tibiae in the fossil record have missing proximal and/or distal epiphysis, and, in fact, there is only one complete tibia in the Middle Pleistocene, the Broken Hill Tibia (E691), in which all these primitive traits are already present but none of the Neanderthal clade (Trinkaus, 2009). Neanderthal-derived morphology in tibiae is defined by wide proximal and distal epiphyses related to bone length, a robust diaphysis, an amygdaloid midshaft shape, and a big distal malleolus. Apart from Broken Hill tibia, *Homo neanderthalensis* is the hominin species, except our own species, in which more complete tibiae specimens are preserved.

Paleoanthropological studies did not use to focus on the fibula because it is the scarcest long bone in the fossil record. This may be because it is a very thin and gracile bone, easily broken on the site by taphonomy or by the excavation itself (Marchi, 2007), and thus difficult to identify, particularly for the early periods of hominin evolution, and possibly confused with a carnivore bone if distal and proximal epiphyses are missing (White et al., 2012). Despite that, several studies have highlighted its importance in understanding locomotor adaptations in extant

TABLE 1 Adult tibiae inventory.

Adults	Side	Description
AT-848	R	Complete
Tib I	R	Almost complete without malleolus
Tib III	L	Almost complete without malleolus nor tuberosity
Tib IV	R	Almost complete without lateral plateau
Tib VI	R	Almost complete
Tib XI	R	Almost complete without malleolus
Tib XII	R	Complete

TIB-I: AT-85 + AT-328.

TIB-III: AT-91 + AT-119 + AT-838.

TIB-IV: AT-438 + AT-439 + AT-440 + AT-3858 + AT-3859.

TIB-VI: AT-1046 + AT-1062 + AT-1073 + AT-1081 + AT-2482 + AT-3997 + AT-4820.

TIB-XI: AT-2138 + AT-2134 + AT-2173 + AT-2213.

TIB-XII: AT-836 + AT-1079 + AT-2199 + AT-2550.

hominids and fossil hominins (Marchi, 2007, 2015; Marchi et al., 2017, 2022; Marchi & Shaw, 2011).

The fibula articulates with the tibia at three different facets: the proximal tibiofibular facet, the distal tibiofibular facet (which is not always present), and the distal fibulotalar facet. Regarding proximal tibiofibular joint, it can be classified into two types horizontal and oblique (Ogden, 1974). The normal inclination in modern humans is 25° and a range between 5° and 60°.

The distal epiphysis of the fibula, together with the distal tibia and talus, forms the ankle joint. This is the most recognizable part of the fibula and the most analyzed in studies of human evolution taken a special value the analysis of the fibulotalar articular facet, as well as the presence of the tibiofibular distal facet and the shape of the subcutaneous triangular surface (STS) (Barnett & Napier, 1953; Marchi, 2015; Marchi et al., 2017, 2022). The shape and location of the STS is thought to be related to the development of the peroneal groove, which is in turn related to the size of the gastrocnemius and soleus muscle bellies (Biewener, 2016; Marchi et al., 2022; Payne et al., 2006). These muscles are active during the support and second half of the stance phase of locomotion in humans (Marchi, 2015). Thus, fibula is used to stabilize the ankle joint in plantigrade locomotion, stability is greatest during dorsi-flexion (Barnett & Napier, 1953).

Neandertal traits of the fibula are those related to epiphyseal and diaphyseal robusticity (Boule, 1911; Heim, 1982; Trinkaus, 1983), but due to the scarcity of this type of skeletal element, there is not much information and detailed descriptions. However, there are some examples of relatively well-preserved fibular elements in the fossil record, although they are not complete. These examples include ARA-VP-6/500 (*Ardipithecus ramidus*, White et al., 2009), AL 288-1 (*Australopithecus afarensis*,

TABLE 2 Tibial measurements for adult representative specimens. Measurements in mm.

		TIB-I	TIB-III	TIB-IV	TIB-VI	TIB-XI	TIB-XII	AT-848
Maximum length	M1a	341	383	329	361	354	371	381
Proximal breadth	M3	69.5	77.0	66.4	79.3	72.0	83.4	77.6
Plateau displacement	T	41.1	46.3	37.8	48.1	43.8	50.8	46.4
Distal epiphysis ML diameter	M6			44.8			55.3	54.0
Anteroposterior diameter at foramen	M8a	36.3	42.3		40.1	42.1	43.3	43.6
Mediolateral diameter at foramen	M9a	24.4	25.0		29.9	28.0	29.0	26.6
Perimeter at the foramen	M10a	91	117		110	112	111	108
Retroversion angle	M12	13.1	15.5	12.0	19.5	14.9	18.8	13.9
Inclination angle	M13	9.3	10.4	8.1	14.9	11.1	14.4	10.2
Torsion angle	M14	23.8	19.9	31.3	23.7	18.1	18.2	20.0

Note: Measurements from M followed by a number that is the measurement for the tibia in Martin and Saller (1957), T = Trinkaus (1983). SH Tibial lengths from Carretero et al. (2012).

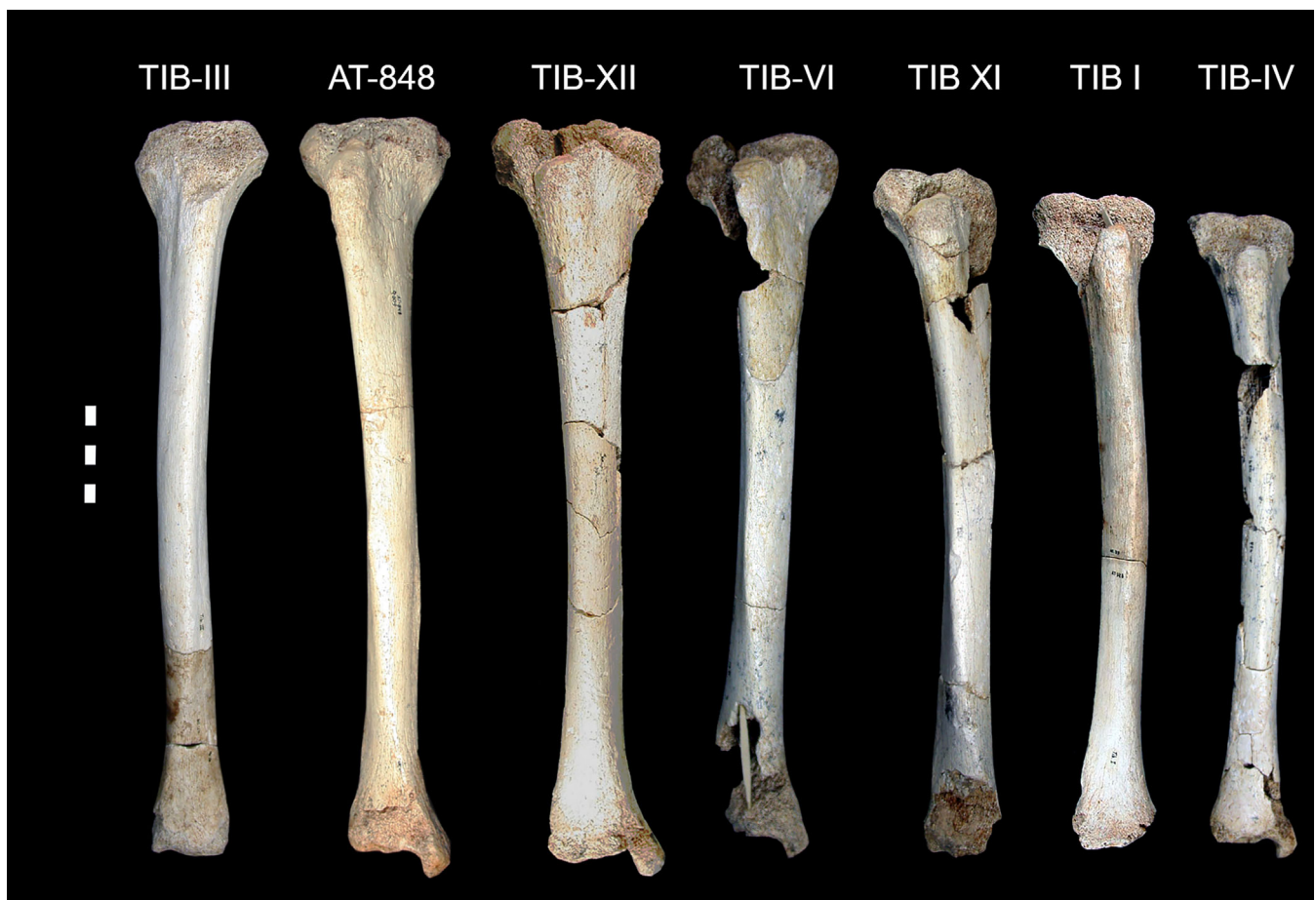


FIGURE 1 Complete or almost complete tibial remains from Sima de los Huesos Site.

Johanson and Taieb, 1976), KNM-ER 1500 (*Paranthropus boisei*, Grine, 1988), OH 35 (*Homo habilis*, Susman, 2008), KNM-ER 1481 (*Homo sp.*, Kennedy, 1983), KNM-WT 15000 (*H. ergaster*, Walker and Leakey, 1991), several fragmental *Homo naledi* specimens (Marchi et al., 2017), and *Homo neanderthalensis* specimens,

including La Ferrassie 1, La Ferrassie 2, Amud-1, Tabun C1, some Krapina remains (Heim, 1982), Kiik-Koba (Trinkaus et al., 2008), and Shanidar (Trinkaus, 1983).

It is known that bone shape is influenced by the tensions experienced during development. As a result, habitual positions and locomotion patterns during growth can



**FIGURE 2** Right TIB-I. Scale bar 5 cm. From left to right: Anterior, medial, posterior, and lateral views.

impact bone morphology (Aiello & Dean, 1990; Mizushima et al., 2016; Trinkaus, 1975). However, this variation can also be attributed to several factors, ranging from nutrition to climatic adaptation and locomotor efficiency (Allen, 1877, Bogin et al., 2002; Higgins & Ruff, 2011). These factors are not necessarily exclusive but may complement each other. Recent analyses of human tibiae, both modern and fossil, suggest that the tibia is particularly sensitive to detecting mobility due to its medial-lateral positioning under the body's center of gravity (Ruff, 2005; Ruff et al., 2006). Furthermore, the robustness of the fibula is considered one of the best indicators not only of the amount of locomotion but also of the direction of habitual loading and ankle mobility (Sparacello et al., 2014). Marchi and Shaw (2011) noted that cross-sectional properties of the fibula, relative to the tibia, seem to be mainly correlated with terrain properties and frequent changes of direction rather than directly reflecting the level of mobility.

Concerning locomotion economy, longer lower limbs have been associated with increased speed, which is likely to have been favored by natural selection due to substantial savings in locomotor costs (Kramer & Eck, 2000; Steudel-Numbers & Tilkens, 2004).



**FIGURE 3** Left TIB-III. Scale bar 5 cm. From left to right: Anterior, medial, posterior, and lateral views.

Additionally, body shape has been identified as an important source of variation. Kramer and Silvestre's (2009) demonstrated that the oxygen volume consumed ( $VO_2$ ) during movement (external power) is dependent on the crural index value, with higher costs associated with lower indices, while the energetic cost of moving the legs (internal power) depends on the individual's circumference (size).

Regarding climate, Blackburn et al. (1999) found that the ecogeographic patterning of human body form cannot be entirely attributed to clinically distributed natural selection. They proposed three different models to explain variation in the crural index in modern humans, with the "structure model" being the best fit. This model is based on the random effect of population structure, suggesting that random genetic drift, mutation, and gene flow play a role in the population's traits. Furthermore, Steudel-Numbers and Tilkens (2004) suggested that Neanderthals' ability to insulate their bodies with clothing was insufficient, and their active lifestyle may have involved activities where shorter limbs were more advantageous than energetic efficiency (such as hunting with spears in even terrain, where powerful legs and



**FIGURE 4** Right TIB-IV. Scale bar 5 cm. From left to right: Anterior, medial, posterior, and lateral views.

a lower center of mass are beneficial). In fact, studies have shown that Neanderthals were heavily muscled, providing them with both greater thermogenic capacity and better insulation against the cold (Aiello & Wheeler, 2003; Churchill, 2006).

The Sima de los Huesos (SH) is a small chamber located deep within an underground karst system in northern Spain's Atapuerca region. It is renowned for being a rich source of fossil hominin specimens, as documented by Arsuaga et al., 2014. To date, over 7000 human fossils from at least 29 individuals have been identified in this collection of commingled hominin remains, as reported by Bermudez de Castro et al. in 2020. These fossils are found within a single stratigraphic level that has been redated to approximately 430,000 years ago (Arsuaga et al., 2015).

While a few fossils have been discovered in close anatomical proximity and are exceptionally well-preserved, the majority of specimens do not exhibit a clear sorting or alignment (Arsuaga et al., 1997). This lack of distinct organization has thus far hindered the skeletal characterization of the individuals in this assemblage. Of these



**FIGURE 5** Right TIB-VI. Scale bar 5 cm. From left to right: Anterior, medial, posterior, and lateral views.

fossil remains, 15% belong to postcranial long bones (851 remains), and of these, 47% are lower limb (leg) bones (393 remains). Of these leg bone remains, 25.4% belong to adult individuals (100 remains), 51.3% belong to subadults (202 remains), and 23.2% (91 remains) cannot be aged. In this paper, we describe adult tibiae and fibulae remains. This allows us to show the variation of the largest sample of tibia and fibula samples belonging to one population of the Middle Pleistocene, so far (Arsuaga et al., 2015).

Substance strategies are a set of actions and measures chosen by hominins in a specific place and at a specific time to obtain the means necessary for survival and reproduction, both as individuals and as a group (Huguet et al., 2013). And although patterns of activity and mobility can be giving us information about those strategies, it is not the aim of this paper to focus in this multifactorial and complex concept, but to offer a hypothesis about activity, energy expenditure and skeletal morphology (Marchi 2007; Marchi & Shaw, 2011; Marchi et al., 2022; Ruff & Hayes, 1983; Trinkaus, 1993; Trinkaus & Ruff, 2012; Ward, 2002).

In any case, and in addition to the SH fossil sample, there is evidence of active procurement of large ungulates through hunting by hominids during the Middle Pleistocene in Gran Dolina TD10, which is also part of the



**FIGURE 6** Right TIB-XI. Scale bar 5 cm. From left to right: Anterior, medial, posterior, and lateral views.



**FIGURE 8** Right AT-848. Scale bar 5 cm. From left to right: Anterior, medial, posterior and lateral views.



**FIGURE 7** Right TIB-XII. Scale bar 5 cm. From left to right: Anterior, medial, posterior, and lateral views.

Atapuerca Sites. Numerous pieces of evidence support this assertion (Rodríguez-Hidalgo et al., 2015, 2016). This site has been dated to a range of approximately 380,000–

**TABLE 3** SH Adult fibulae inventory.

Label	Side	Description
FIB-I	L	Complete
FIB-II	L	Complete
FIB-III	L	Complete bone except proximal end
FIB-IV	R	Complete bone except proximal end
FIB-V	R	Complete bone except proximal end
FIB-VI	L	Complete
FIB-VII	L	Distal third
FIB-VIII	L	Complete
FIB-IX	R	Distal third plus midshaft
FIB-X	L	Distal two-thirds

FIB-I: AT-2469 + AT-2561 + AT-2562.

FIB-II: AT-309 + AT-1739 + AT-4254 + AT-1519.

FIB-III: AT-3309 + AT-3304 + AT-1058 + AT-5165.

FIB-IV: AT-880 + AT-1059 + AT-3468 + AT-3968.

FIB-V: AT-3306 + AT-4247 + AT-1724 + AT-1708 + AT-3989.

FIB-VI: AT-1060 + AT-1061 + AT-1121.

FIB-VII: AT-3310 + AT-3305 + AT-3324.

FIB-VIII: AT-4396 + AT-5600 + AT-5601 + AT-6187.

FIB-IX: AT-1936 + AT-2475.

FIB-X: AT-6837 + AT-6851 + AT-6891 + AT-6892.

TABLE 4 Adult SH fibulae measurements in millimeters.

		FIB-I	FIB-II	FIB-III	FIB-IV	FIB-V	FIB-VI	FIB-VII	FIB-VIII	FIB-IX	FIB-X
Maximum length	M-1	353	330	357							
Proximal epiphysis mediolateral diameter	M-4.1	26.4	23.4								
Minimum proximal perimeter	M-4a	50.0	40.0				38		41		
Maximum proximal diameter	T	17.3	15.0				14.8		12.5		
Minimum proximal diameter	T	12.7	10.6				11.6		11.1		
Mediolateral diameter at midshaft	M-3.1	15.2	12.6	12.5	14.2	15.7	16.9		15.5		14.1
Anteroposterior diameter at midshaft	M-3.2	17.7	13.2	15.5	13.1	13.2	13.2		14.4		14.2
Minimum perimeter at midshaft	M-4	51.0	43.0	44.0	44.0	43.0	47.0		47.0		46.0
Distal epiphyseal breadth	M-4.2		17.8	18.1	19.7	17.0	18.1	18.4		21.0	
Distal depth	T	31.3	24.7	26.0	28.4	26.9	28.2	25.0		30.4	
Articular distal depth	T	27.2	18.9	17.4	18.9	19.2	20.0	20.1		21.2	
Articular distal height	T	22.5	22.4	24.2	24.4	25.0	26.2	20.5		24.5	

Measurements from M followed by a number is the measurement for the fibula in Martin and Saller (1957), T = Trinkaus (1983).

458,000 years ago, as determined by ESR mean data (Saladié et al., 2018). Furthermore, all the lithic material discovered in this specific layer is of local origin and is found within a maximum distance of 5 km from the site (Terradillos and Rodríguez-Alvarez, 2014).

The aim in this paper, is then, to introduce the tibiae and fibulae SH remains and to detect some morphometric traits which define the population. Also, to contribute to the creation of an illustrated catalog of SH specimens to allow the comparison to other fossil specimens, and to give measurements and basic statistics and the possible significance of some important morphometric traits described here related to biomechanics and energetic cost.

## 2 | MATERIALS AND METHODS

### 2.1 | Sima de los Huesos sample

In SH site we have recovered 104 tibiae-labeled fragments representing 10 adult elements, taking into consideration the proximal end and size incompatibilities. From this, the minimum number of individuals (MNI) can be determined as six adult individuals represented by tibiae. Furthermore, there are 106 labeled fragments that correspond to fibulae, which form 10 adult elements and represent the NMI of seven adult individuals, as represented by fibula distal epiphysis.

We provide detailed pictures of the bones and features based on the original specimens from SH. We do

not report detailed anatomical descriptions of every specimen, only highlighting the main anatomical features representing the whole sample based on adult specimens. Additionally, we report an inventory of the most complete specimens. All labeled fragments are named as AT (i.e., Atapuerca, Sima de los Huesos) followed by an Arabic number (e.g., AT-848). We give a bone number, represented by “TIB” for the tibiae and “FIB” for the fibulae, only when the distal half for the tibiae is present and distal epiphysis for the fibula.

### 2.2 | Tibial SH inventory and minimum number of individuals

Table 1 contains the inventory of the more significant specimens, while Table 2 includes only some of the main dimensions used to characterize the SH tibia in the most complete adult specimens. Figure 1 displays the most complete tibial remains from the SH sample. Figures 2–8, offer the anatomical views of these complete specimens.

### 2.3 | Fibula SH inventory and MNI

Table 3 contains the inventory of only most complete specimens. Table 4 shows the main dimensions from adult individuals. Figure 9 displays the most complete fibulae remains from SH sample, and Figures 10–16, offer the anatomical views of these more complete specimens.



FIGURE 9 Complete or almost complete fibula remains from Sima de los Huesos site.

## 2.4 | Comparative sample

In Table 5 we give the details of the comparison sample. We have studied various Neanderthal specimens, including the originals of La Ferrassie 1 and 2 (Tibia and fibula), and La Chapelle-aux-Saints 1 (Tibia), all housed in the Musée de l'Homme in Paris, as well as the cast of Spy2 (Tibia). Data on other fossils were derived from different bibliographic sources, such as Kiikoba tibia (Heim, 1982) the Shanidar tibiae and fibulae (Trinkaus, 1983), Tabun C1 (Fibula, Trinkaus, 1983). Beside these,

Broken Hill (Tibia, Trinkaus, 2009). Boxgrove (Tibia, Lockey et al., 2022), and also some Lower Pleistocene individuals, such as the Daka tibiae (Gilbert, 2008) or Nangdong (Antón, 2003) for which morphological traits are also used.

In addition to these fossil specimens, we also studied several modern human samples for both bones, tibiae and fibulae. The first comparative sample called the “Portuguese sample,” was drawn from individuals belonging to collections housed in the Bocage Museum (National Museum of Natural History, Lisbon, Portugal)



**FIGURE 10** Left FIB-I Scale bar 5 cm. From left to right: Anterior, medial, posterior, and lateral views.

and the Department of Life Sciences at Coimbra University (Coimbra, Portugal). Both collections are formed by Portuguese people who lived in the nineteenth and twentieth centuries and represent the middle-to-low social class of the cities of Lisbon and Coimbra (Cardoso, 2006; Coquegniot & Weaver, 2007).

The second sample is composed of individuals from the Hamann–Todd collection housed in the Cleveland Museum of Natural History in Ohio (USA) and the Forensic Data Bank (Jantz & Moore-Jansen, 2000). This sample was divided into two subsamples based on whether the individuals were African American or had European ancestry.

The third sample is composed of individuals from the archeological collection from San Pablo (Burgos) housed in the Laboratory of Human Evolution. In these recent humans individuals, sex was estimated based on non-metric traits of the skull and pelvis using the standard described in Buikstra and Ubelaker (1994), these are Acsadi and Nemeskeri (1970) for the skull, and Phenice (1969) for the coxa.



**FIGURE 11** Left FIB-II Scale bar 5 cm. From left to right: Anterior, medial, posterior, and lateral views.

## 2.5 | Measurements

Here, we are providing those basic measurements from both SH tibiae and fibulae remains following Martin and Saller (1957), Trinkaus (1983), and Carretero et al. (2012). We used standard anthropological techniques and instruments, including Mitutoyo digital calipers and osteometry boards for linear measurements, to take all measurements in the SH specimens and our comparative samples. In addition, tibial plateau displacement was measured as in Trinkaus (1983) and used in Trinkaus and Rhoads (1999) through a photograph taken in medial view. It was measured at the point where the Maximum AP diameter at the tibial tuberosity (Martin & Saller, 1957 measurement 4) intersects a perpendicular line in the tibial tuberosity with a sliding caliper. Then, we calculated the projected distance between that line



**FIGURE 12** Left FIB-III Scale bar 5 cm. From left to right: Anterior, medial, posterior and lateral views.

and the intercondylar tubercle (spines; Figure 17a). STS length is measured from the distal tip of the lateral malleolus in anterior view of the fibula to the point where the anterior ridge divides into two ridges, landmarks 1 and 4 in Marchi et al. (2022).

Retroversion and inclination tibial angles were measured using pictures and AUTOCAD software (Autodesk, 2012) as recommended by Martin and Saller (1957, measurements 12 and 13). In the medial view, we drew the anatomical and mechanical axis based on Olivier's method (Olivier, 1969), and then measured the retroversion and inclination angles relative to the medial tibial plateau inclination with these two axes (Figure 17b, c).



**FIGURE 13** Right FIB-IV Scale bar 5 cm. From left to right: Anterior, medial, posterior, and lateral views.

Tibial torsion angle was measured using a proximal view picture, with the distal articulation axis fixed in the horizontal plane. We measured the angle between the distal articulation axis (axis drawn with distal articular breadth measurement, Trinkaus, 1983) and proximal articulation axis (axis drawn with proximal breadth measurement, M3) as recommended by Martin and Saller (1957, measurement 14), using AUTOCAD software (Autodesk, 2012; Figure 17d).

STS length was measured as the linear distance between the most distal point of the lateral malleolus in the anterior view and the point where the anterior ridge divides into two ridges. These two points are defined as landmark 1 and 4 in Marchi et al. (2022).



**FIGURE 14** Right FIB-V Scale bar 5 cm. From left to right: Anterior, medial, posterior and lateral views.

Finally, we want to notify that there are some differences in the section modulus values between those calculated with Autocad software, as we did in Rodríguez et al. (2018), and the same values calculated with Moment-Macro software (C. B. Ruff personal communication). Due to most people using Moment-Macro, we offer in Table 6, the new SH section modulus values at midshaft of the tibia and fibulae calculated with this software.

Basic Statistical analysis were performed through SPSS v 26 software (Meulam & Heiser, 2019). For species comparison, all variables for each sample were tested for normality. Because normality cannot be assumed in all of the variables, and in order to be coherent with all the comparison analysis, Kruskal–Wallis test was chosen followed by a U-Mann–Whitney test, when necessary.



**FIGURE 15** Left FIB-VII Scale bar 5 cm. From left to right: Anterior, medial, posterior, and lateral views.

### 3 | RESULTS

#### 3.1 | Tibiae anatomical clues

Table 7 shows the basic statistics and the comparisons with Neanderthals and modern human samples tibiae and Table 8 shows the description and possible polarity of tibial trait evolution patterns relative to a standard modern



**FIGURE 16** Left FIB-X Scale bar 5 cm. From left to right: Anterior, medial, posterior, and lateral views.

human tibia. The most important anatomical traits are displayed in Figures 18 and 19. The SH specimens are characterized by having a wider proximal epiphysis than recent modern humans (Figure 18a and Table 3), a tibial tuberosity that is more projected forward and lateral than in recent modern humans (Figure 18b), or in other words, the tibial plateau is shifted backward (Figure 18c) The tibial plateau exhibits moderate retroversion (Figure 18d), with a medial retroversion angle of  $18^\circ$ .

In the anterior view, SH specimens display medial buttressing of the tibial proximal metaphysis (Figure 18e), Additionally, they have a large distal epiphysis and malleolus (Figure 18f and Table 7), similar to

Neanderthals, although the differences are within the variability of modern humans (Table 7). The squatting facet is variable, although it is absent in TIB-III, TIB-XII, and AT-848, it can be detected in TIB-I and TIB-IV, and there is a lack of bone substance in some of the specimens (TIB-VI and TIB-XI).

In terms of the diaphysis, in the anterior view, SH specimens have a proximally curved bone (Figure 18g), which is different from those of modern humans and other fossil specimens such as Daka, Broken Hill, and Boxgrove. In the medial and lateral views, they have a posteriorly and angled displaced plateau (Figure 18d, and see retroversion and inclination angle values in Table 2). There are statistical differences in the platymeric index; SH tibiae are similar to Neanderthals but more platymeric than modern humans (Figure 18h and Figure 20, Table 3). They also have a distal asymmetric notch for the fibula (Figure 18i), with the posterior border less projected and horizontal than in *Homo sapiens*. Furthermore, there is a well-developed tibial pilaster (Figure 18j).

In the proximal view, the torsion angle (Table 2) falls within the range of variation observed in modern humans ( $N = 45$ ,  $30.3^\circ \pm 5^\circ$ ) by Jakob et al. (1980) and in a range among  $0^\circ$ – $40^\circ$  by Aiello and Dean (1990) and some other hominins, such as Broken Hill ( $15^\circ$ ). The proximal epiphysis has a thick and continuous intercondylar eminence (Figure 19a), with a sharp anterior cruciate ligament insertion (Figure 19b), a large fossa for the anterior cruciate ligament (Figure 19c), and a wider transverse ligament area than in modern humans (Figure 19d). In the distal view, the tibia is characterized by a more rectangular distal epiphysis (Figure 19e), with a less projected and straighter lateral border of the anterior surface of the fibular notch (Figure 19f). The morphology of the inner malleolus is variable, with some specimens exhibiting a more perpendicular wall to the articular talar surface similar to modern humans, while others are more medially projected as in Neanderthals (Figure 19g).

Lastly, the tibiae have thick cortices with an amygdaloid shape (Figure 18k and see Rodríguez et al., 2018), similar to Neanderthals but different in shape to other Middle Pleistocene human remains such as those from Boxgrove and Broken Hill. Due to the differences in the calculus of section modulus between Autocad and Momentmacro software, new section modulus values at midshaft are provided for these tibiae in order to compare with those published by others (Table 6).

### 3.2 | Fibulae anatomical clues

SH fibulae can be described as bones with a large proximal epiphysis (Figure 21a) and a small styloid process

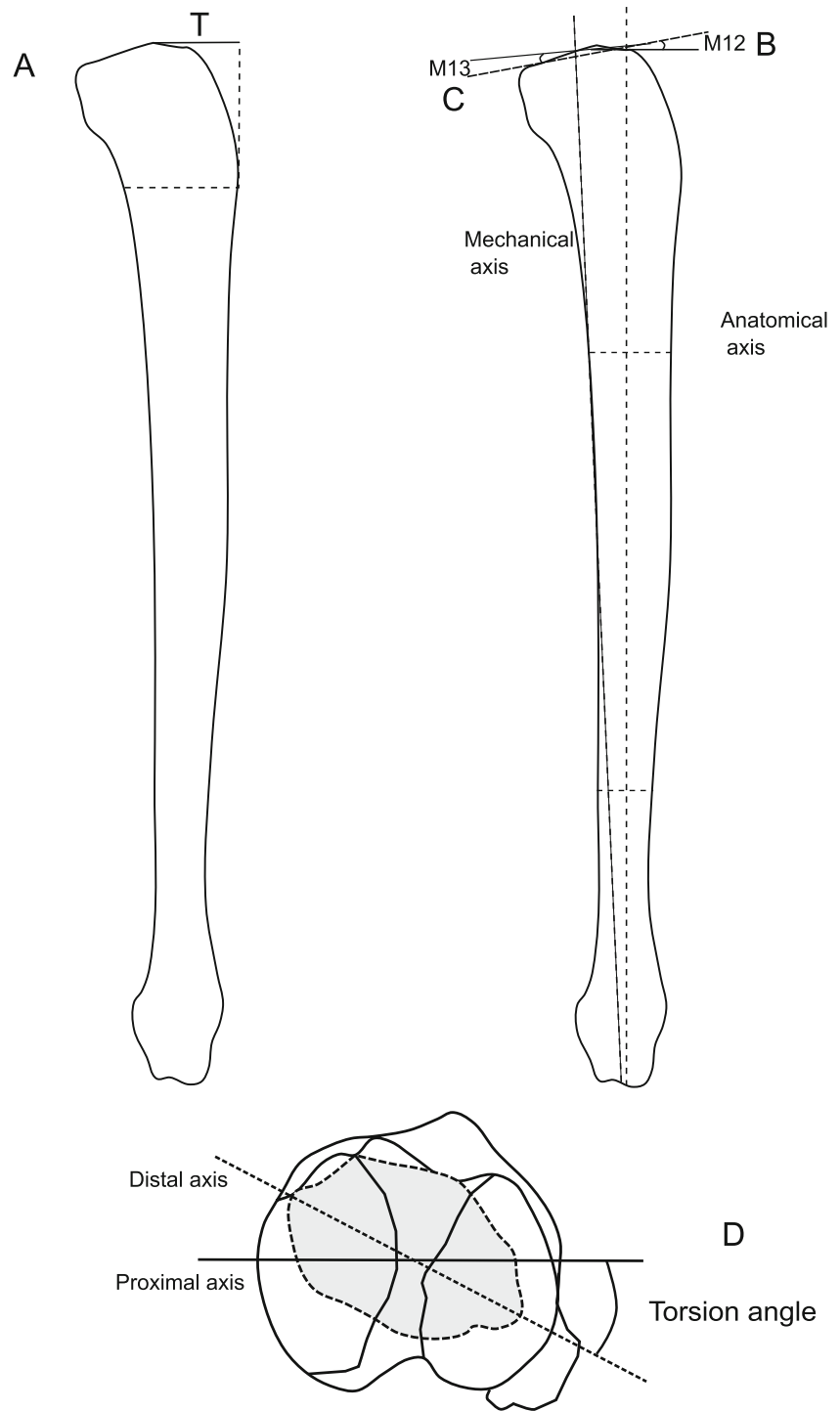
TABLE 5 Comparison sample for tibia and fibula used in this study.

	Species	Collection/ specimen	Origin	N	Source	Location	
TIBIA	<i>H. sapiens</i>	Portuguese sample	Europe	130	This study	Coimbra University and Lisboa Natural History Museum (Portugal)	
		San Pablo (Spain)	Europe	200	This study	Laboratorio de Evolucion Humana. Universidad de Burgos (Spain)	
		Forensic Data Bank	African	260	Jantz and Moore-Jansen (2000)	Forensic data Bank, Tennessee (USA)	
			American	480			
	Hammand Todd	Europe	30	This study	Cleveland Natural History Museum (USA)		
		African American	30				
	<i>H. neanderthalensis</i>	La Ferrassie-1	France	1	Originals and Heim, 1982	Museum de L'Homme (Paris)	
		La Ferrassie-2	France	1	Originals and Heim, 1982	Museum de L'Homme (Paris)	
		La Chapelle aux-Saints	France	1	Originals and Heim, 1982	Museum de L'Homme (Paris)	
		Kiikoba		1	Heim, 1982		
		Spy 2	Belgium	1	Cast	Museum de L'Homme (Paris)	
		Middle Pleistocene	Kabwe/Broken Hill	Zambia	1	Trinkaus, 2009	
			Daka	Etiopia		Gilbert, 2008	
			Ngandong 13B	China	1	Antón, 2003	
	Boxgrove	England	1	Stringer et al., 1998			
FIBULA	<i>H. sapiens</i>	Portuguese sample	Europe	103	This study	Coimbra University and Lisboa Natural History Museum (Portugal)	
		Forensic Data Bank	African	176	Jantz and Moore-Jansen (2000)	Forensic data Bank, Tennessee (USA)	
			American	312			
	San Pablo (Spain)	Europe	82	This study	Laboratorio de Evolucion Humana. Universidad de Burgos (Spain)		
	<i>H. neanderthalensis</i>	La Ferrassie 2	France	1	Originals and Heim, 1982	Museum de L'Homme (Paris)	
		Tabun C1	Israel	1	Trinkaus, 1983		
		Shanidar 6	France	1	Trinkaus, 1983		
		La Ferrassie 1	France	1	Originals and Heim, 1982	Museum de L'Homme (Paris)	
		Kiik-Koba	URSS	1	Cast	Museum de L'Homme (Paris)	
		Shanidar 1	Iraq	1	Trinkaus, 1983		
	Shanidar 2	Iraq	1	Trinkaus, 1983			

(Figure 21b). Relative to the diaphysis, and because this bone is affected by minor variations in sural muscles (Trinkaus, 1983), they have a variable development of muscular crests (Figure 21c), high diaphyseal

robusticity (Figure 21d), high neck robusticity diaphysis (Figure 21e), a minimum proximal perimeter located distally (Figure 21f), a straight diaphysis (Figure 21g), and thick cortices (Figure 21h). Finally, concerning the

**FIGURE 17** Tibial Plateau displacement (a), Retroversion (b) and inclination angles (c), Torsion angle (d). Tibial Plateau displacement (a: Trinkaus, 1983) projected distance between that line and the intercondylar tubercle (spines). Retroversion (b: M12): Angle formed by the plane of the condyle or tibial plateau with respect to the perpendicular to the anatomical axis of the tibia. Anatomical axis (Olivier, 1969): Axis that passes through the midpoint of the diaphysis at the level of the nutrient foramen and halfway at any level of the distal diaphysis. Inclination (c: M13): Equivalent to retroversion, but passing through the mechanical axis of the tibia. Mechanical axis (Olivier, 1969): Axis that passes through the center of the two proximal and distal articular surfaces, taken in this case from a medial view. Tibial torsion angle (d: M14) was measured using a proximal view picture, with the distal articulation axis fixed in the horizontal plane.



distal epiphysis, they have a flatter mediolaterally distal epiphysis than modern humans (Figure 21i) due to a bigger anteroposterior diameter (Figure 21j), a short malleolar fossa (Figure 21k, l), an elliptical-shaped and antero-superiorly sloped distal articular surface (Figure 21m), with little development of the lateral malleolus (Figure 21n) and an STS which are statistically below modern human mean (Figure 21p, Table 9). There is variable presence of the distal tibiofibular

articular facet (Figure 21o), Fib-II and Fib-VII have this facet, while Fib-III, Fib-IV, Fib-V, Fib-VIII, Fib-IX, and Fib-X do not. We cannot be sure about Fib-I due to its poorly preserved state. Therefore, the percentage of its presence in SH is around 25%. There are only two proximal epiphyses of the SH fibulae in which proximal tibiofibular angle can be measured, Fibula I (19°) and Fibula II (35°), which fall inside the modern human range. Table 10 shows the description and possible

		SECTION	Zx	Zy	Zp
TIBIA	AT-848	50%	2648.7957	1669.054	3688.888
	TIB-I	50%	1529.1731	1206.6673	2388.9485
	TIB-III	50%	2571.4362	1564.1976	3522.2838
	TIB-IV	50%	1139.0127	924.9895	1809.819
	TIB-VI	50%	2110.3665	1613.0314	3263.3398
	TIB-XI	50%	1966.3847	1389.2973	2772.4812
	TIB-XII	50%	2793.465	1733.1156	3786.0383
FIBULA	FIBIII	50%	216.9272	142.4186	317.6214
	FIBII	50%	173.8755	136.9941	284.4253
	FIBI	50%	311.5603	229.2958	497.0702
	AT-1060	50%	230.9767	172.1406	359.4253

**TABLE 6** Tibia and fibula section modulus calculated with MomentMacro. Measurements in mm<sup>3</sup>.

polarity of fibular traits in relation to a standard modern human fibula.

## 4 | DISCUSSION

In this paper, we present one of the biggest samples of tibiae and fibulae in the fossil record and compare them to modern humans and Neanderthals. This collection is in the Neandertal roots (Arsuaga et al., 2014) and thus we can check if their tibia and fibula are already similar to Neandertals or if they are still sharing the primitive model of *Homo erectus/ergaster*.

### 4.1 | Tibia morphology

Regarding the tibia, proximal and distal epiphysis are bigger than modern humans and similar to those of Neandertals. Thus, it looks like the large articulations that characterize the Neandertals are already present in those Middle Pleistocene populations and in the whole skeleton, as was settled in Arsuaga et al. (2015) and other papers in this present volume (Carretero et al., 2024a, 2024b; García-González et al., 2024; Rodríguez et al., 2024).

In medial and lateral views, they have a posteriorly and angled displaced plateau (Figure 18d, and see retroversion and inclination angle values in Table 2). This trait is shared with Neanderthals (which also have thick patella), Broken Hill, and archaic *Homo sapiens*, and it implies greater knee stability (Trinkaus & Rhoads, 1999). This trait is not unique to Neanderthals but is a primitive character shared by all Pleistocene individuals (Aiello & Dean, 1990; Trinkaus, 2009) and present in all SH specimens. The

shape is related to the tensions experienced during development, where tensional forces accelerate epiphyseal growth while compression forces retard it. This configuration displaces the *m. quadriceps femoris* tendon anteriorly relative to the distal femur increasing the anteroposterior distance between the patellar ligament and the primary flexion-extension axis of rotation of the knee, increasing the moment arm for the quadriceps femoris (Trinkaus & Rhoads, 1999). Besides, habitual positions and locomotion patterns during growth can affect this trait (Aiello & Dean, 1990; Trinkaus, 1975).

In addition, the retroversion angle is similar to those of late Pleistocene archaic humans ( $15.4^\circ \pm 1.7^\circ$ ,  $n = 5$ ), as well as many non-mechanized recent human samples (Trinkaus, 1975; Trinkaus & Rhoads, 1999). Torsion angle is also inside modern human variation range, and it is related to the way of walking (Hicks et al., 2007). The highest mean of the torsion angle value in SH hominins can imply a slower speed in walking (Schwartz & Lakin, 2003). So regarding the tibiae, the SH hominins could have a normal way of walking, as well as recent modern humans without pathologies.

SH, Neandertal, and Boxgrove tibiae exhibit a strong tibial pilaster, which appears to be absent in Broken Hill and Daka or other Early *Homo* specimens that are characterized also by a subtle interosseous crest (Gilbert, 2008).

### 4.2 | Tibia bone length

Due to the difficulties in properly measuring tibial length in a uniform way, as reported by many authors and explained in the Supplementary information of Carretero

**TABLE 7** Basic statistics for adult tibiae of Sima de los Huesos (SH), Neanderthals, and modern humans, including normality and Kruskal Wallis test with post hoc Mann–Whitney U when necessary.

	Valid	Mean	SD	Normality		Kruskall–Wallis		Post-hoc: U–Mann Whitney			
				SW	p-value	KW	p-value	SH- <i>Homo sapiens</i>	SH-Neanderthals	SH-Neanderthals- <i>H. sapiens</i>	
Maximum length (M1a)											
<i>H. sapiens</i>	1030	368.52	32.82	1.00	< 0.01	3.95	0.139				
Sima de los Huesos	14	354.71	20.26	0.89	0.068						
Neanderthals	5	341.40	28.07	0.96	0.817						
Proximal breadth (M3)											
<i>H. sapiens</i>	976	73.56	6.47	0.98	< 0.01	12.36	< 0.01	0.038	0.298		< 0.01
Sima de los Huesos	14	75.10	5.63	0.93	0.297						
Neanderthals	4	81.50	5.78	0.97	0.84						
Tuberosity projection (T)											
<i>H. sapiens</i>	187	36.34	3.96	0.99	0.7	21.55	< 0.01	< 0.01	0.657		< 0.01
Sima de los Huesos	14	43.61	3.42	0.77	< 0.01						
Neanderthals	5	44.83	7.72	0.95	0.755						
Distal epiphysis ML diameter (M6)											
<i>H. sapiens</i>	981	48.57	4.94	0.99	< 0.01	3.18	0.204				
Sima de los Huesos	6	51.37	5.12	0.72	< 0.01						
Neanderthals	3	50.95	2.62	0.91	0.421						
Anteroposterior diameter at foramen (M8a)											
<i>H. sapiens</i>	1028	27.30	4.70	0.98	< 0.01	23.42	< 0.01	< 0.01	0.498		< 0.01
Sima de los Huesos	12	41.28	2.60	0.79	< 0.01						
Neanderthals	5	36.88	2.85	0.84	0.164						
Mediolateral diameter at foramen (M9a)											
<i>H. sapiens</i>	1049	30.62	6.09	0.97	< 0.01	17.53	< 0.01	< 0.01	0.62		< 0.01
Sima de los Huesos	12	27.15	2.10	0.90	0.141						
Neanderthals	5	26.55	1.47	0.89	0.373						
Perimeter at the foramen (M10a)											
<i>H. sapiens</i>	808	91.03	9.72	0.99	< 0.01	19.14	< 0.01	0.01	0.795		< 0.01
Sima de los Huesos	12	108.17	8.52	0.76	< 0.01						
Neanderthals	4	98.25	6.85	0.88	0.332						

(Continues)



TABLE 8 Tibial trait polarity.

Trait	Non-hominin apes	<i>Au. afarensis</i>	<i>Au. sediba</i>	<i>Homo habilis</i>	<i>H. georgicus</i>	<i>H. naledi</i>	Middle Pleistocene non-SH	SH	<i>Neanderthals</i>	<i>H. sapiens</i>
Proximal condyle shape	Short and unnotched	Short and unnotched	Small notched					Notched		Notched
Plateau inclination	Slope	Sloped?	Sloped?	Sloped?			Sloped	Sloped	Sloped	< slope
Tibial tuberosity	Projected	Projected?		Projected?			Project	Projected	Projected	< projected
Tibial tuberosity groove	Sloped	Horizontal and curved					Horizontal and curved	Horizontal and curved		Horizontal and curved
Tibial plateau location	Posterior						Posterior	Posterior	Posterior	
Groove for the semimembranosus	Circular/tear-drop	Tear-drop/conical								Horizontal groove
Groove for gracilis	Elongated	Elongated		Elongated						Soft
Lateral side of tuberosity	Sharp and hollowed out	Sharp and hollowed out			Gentle curved		Gentle curved	Gentle curved	Gentle curved	Gentle curved
Tibial epicondyles	Narrow	Narrow					Massive	Massive	Massive	Massive
Tibial plateau appearance	Shelf-like	Shelf-like					~ <i>H. sapiens</i>	~ <i>H. sapiens</i>	~ <i>H. sapiens</i>	~ <i>H. sapiens</i>
Shaft				Weak			Weak	Weak	Weak	Vertical, weak
Interosseous crest	Slants forward						Weak marked	Weak marked	Weak marked	Strongly marked
Soleus crest	Not roughened						Weak marked	Weak marked	Weak marked	Strongly marked
Curvature	Continuous concave lateral	Continuous concave lateral		Concave-Convex	Concave-Convex		Concave-convex	Concave-convex	Concave-convex	Concave-Convex
Anterior crest curvature	Curved	Curved		Curved	Curved		Straight	Curved	Curved	Straight
Robusticity (relative to bone length)	Robust			Robust	Robust		Robust	Variable	Robust	
Mid shaft shape	Oval, anteriorly soft			Oval, anteriorly soft	Oval		Oval	Oval	Amigdaloid	Triangle/amigdaloid
Platycnemic	Round			Marked	Marked		Marked	Marked	Marked	Variable
Posterior pilaster	No present			Well developed	Well developed		Well developed	Well developed	Well developed	Well developed

(Continues)

TABLE 8 (Continued)

	Non-hominin apes	<i>Au. afarensis</i>	<i>Au. sediba</i>	<i>Homo habilis</i>	<i>H. georgicus</i>	<i>H. naledi</i>	Middle Pleistocene non-SH	SH	<i>Neanderthals</i>	<i>H. sapiens</i>
Distal Tibiotalar joint slope relative to long axis anterior view	Lateral inclination	Perpendicular	Perpendicular	Perpendicular	Perpendicular	Perpendicular	Perpendicular	Perpendicular	Perpendicular	Perpendicular
Tibiotalar joint slope relative to long axis lateral view	Variable	Variable	Neutral	Neutral	Anteriorly	Anteriorly	Anteriorly	Anteriorly	Anteriorly	Anteriorly
Tibiotalar joint shape	Trapezoidal	Squared	Squared	Squared	Squared	Squared	Squared	Rectangular	Rectangular	Squared
Torsion	Low	Medium	Thick	Thin	Thin	Thin	Thin	Thick	Thick	Small/Thin
Malleolus from distal	Medium	Thick	Thin	Thin	Thin	Thin	Thin	Thick	Thick	Small/Thin
Malleolar slope from distal							Perpendicular	Perpendicular	Sloped	Sloped

Shading boxes mean: Without data.

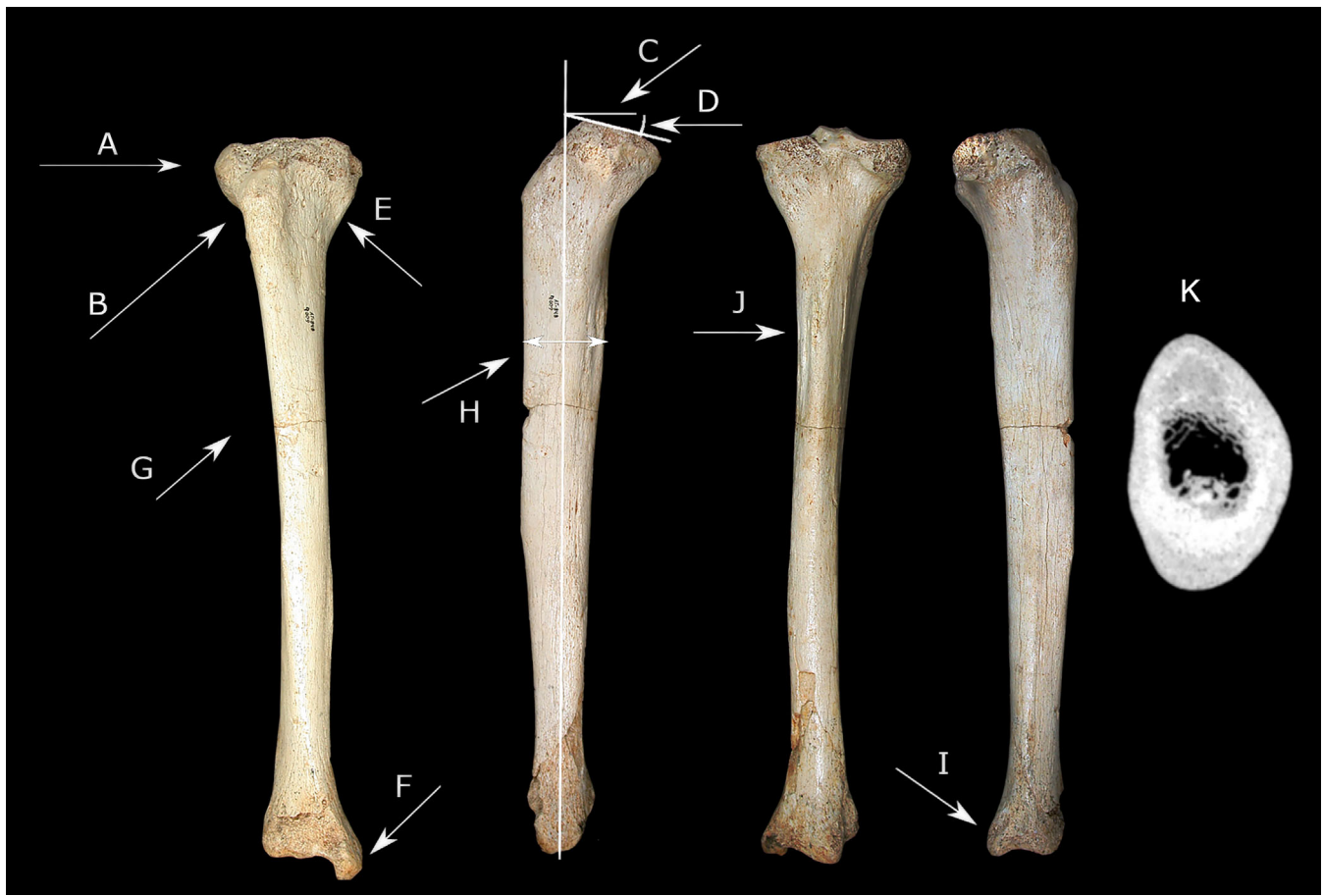


**FIGURE 18** SH main tibial traits. (a) Wider proximal epiphysis, (b) Tibial tuberosity projection, (c) Tibial plateau displacement, (d) tibial plateau retroversion; (e) tibial medial buttressing of proximal metaphysis, (f) large distal epiphysis and malleolus, (g) curved diaphysis, (h) platymeric diaphysis, (i) distal asymmetric notch for the fibula, (j) well-developed tibial pilaster, (k) amygdaloid diaphyseal shape.

et al. (2012), in this paper, we will only use the Maximum length (M1a, Martin & Saller, 1957).

It is known that Neanderthals have shorter tibial lengths relative to body size or relative to femur length, meaning they have lower distal to proximal limb proportions than early anatomically modern humans (Trinkaus, 1981; Holliday, 1997). These low crural indices through load arm shortening, increased the mechanical advantage of their quadriceps muscles via a larger moment arm (Higgins & Ruff, 2011; Trinkaus & Rhoads, 1999).

We expected that this was a common trait shared between SH and Neanderthals, but this pattern of shortening distal limbs may not be present in SH specimens due to tibiae are absolutely longer than those of Neanderthals (Carretero et al., 2012). Therefore, they resemble modern humans and other middle Pleistocene specimens, such as Broken Hill (Trinkaus, 2009) and the estimated value of Boxgrove (Roberts et al., 1994; Stringer et al., 1998). So far, there are no leg bone

associations found at the SH site. Nevertheless, we can assume that, due to an absolute longer tibiae than Neanderthals, at least some SH individuals are going to have longer legs and potentially be taller than Neanderthals, as demonstrated by Carretero et al. (2012). As Holliday (1999) stated, this could be an example of mosaic evolution since overall limb length, brachial, and crural indices appear to have evolved at different rates. Other studies have also suggested a strong genetic component to the development of human body proportions (Auerbach & Sylvester, 2011; Bogin & Ríos, 2003; Frelat & Mitteroecker, 2011; Holliday & Falsetti, 1995), which is likely also the case for SH and Neanderthals. If that higher tibial length in SH individuals is or not related to a higher crural index is something that we take in mind for future studies when we can obtain certain bone associations.

Relative to locomotion economy, Neanderthals, with larger bodies and lower crural indices, would require more energy than modern humans to move (Froehle &

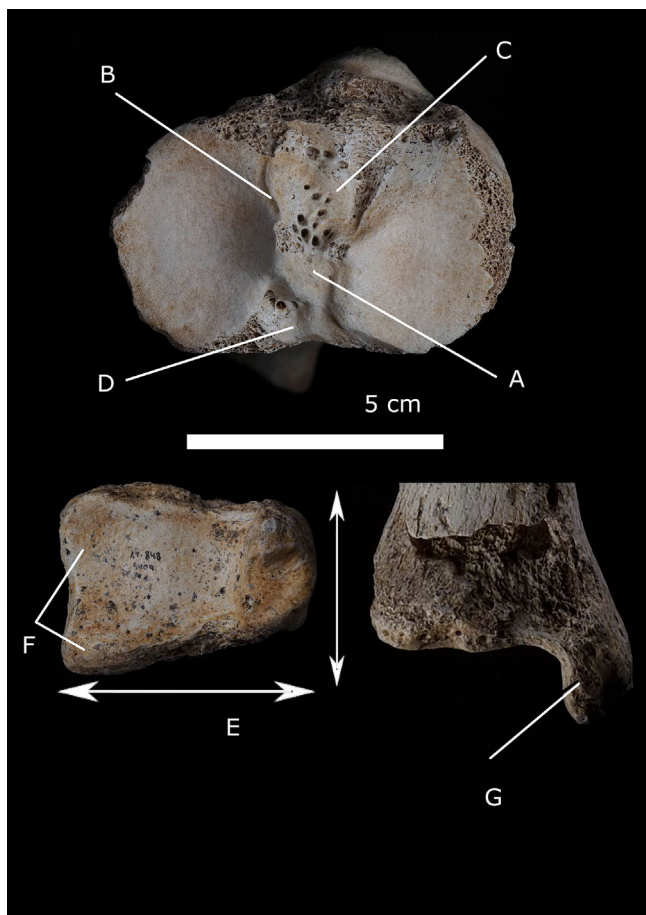


**FIGURE 19** SH epiphyseal tibial traits. (a) Thick and continuous intercondylar eminence, (b) sharp anterior cruciate ligament insertion, (c) large fossa for the anterior cruciate ligament, (d) wider transverse ligament area, (e) rectangular distal epiphysis, (f) less projected and straighter lateral border of the anterior surface of the fibular notch (g) inner malleolus shape is variable.

Churchill, 2009). And if SH specimens have long legs, but similar body weight (Arsuaga et al., 2015) for SH individuals than in Neanderthals, they can be in between modern humans and Neanderthals, in questions of energy cost. Real values of crural indices and associations with patellar remains are needed to answer questions about walking and energy efficiency.

Regarding climate, if ecogeographic model developed by Blackburn et al. (1999) is correct the Neanderthal body shape with relatively short tibiae (Holliday, 1997, 1999; Trinkaus, 1983; Weaver, 2009) should also be a byproduct of their genetic heritage within their own species, rather than a climate adaptation, and individuals may vary their angular motion to accommodate their morphology (Kramer & Silvestre, 2009).

Furthermore, Steudel-Numbers and Tilkens (2004) have suggested that the ability of Neanderthals to insulate their bodies with clothing was not sufficient, and

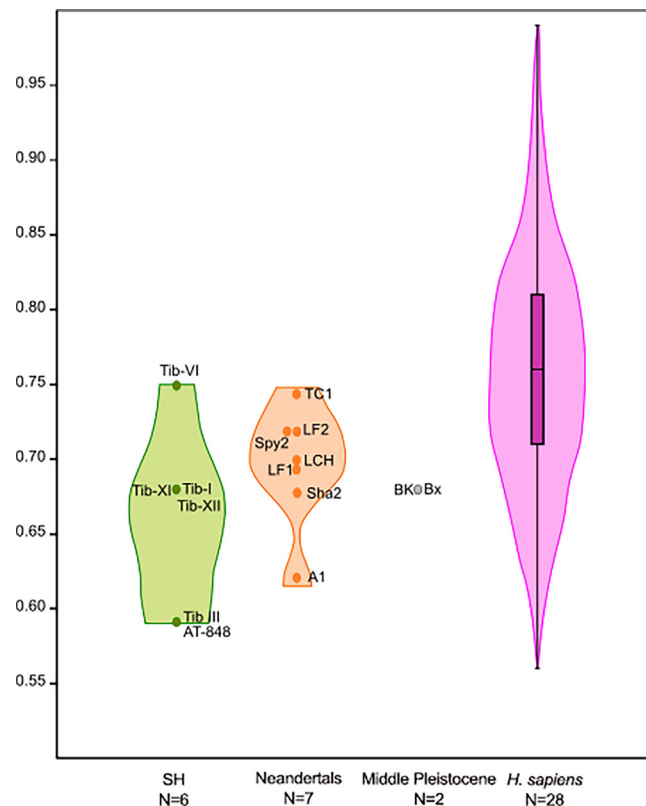


**FIGURE 20** Platymeric index violin graph. Green SH specimens, Orange neanderthals, pink modern humans and gray Boxgrove and Broken Hill tibiae.

their active lifestyle may have involved activities in which shorter limbs were more important than energetic efficiency (such as hunting with spears in even terrain, where more powerful legs and a lower center of mass are beneficial). In fact, it has been shown that Neanderthals were heavily muscled, which may have provided them with both greater thermogenic capacity and greater insulation against the cold (Aiello & Wheeler, 2003; Churchill, 2006), and a good adaptation to their hunting strategy which was focused on terrestrial herbivores (Churchill, 1998; Richards et al., 2000; Villa & D'errico, 2001).

Thus, SH individuals with longer tibiae and posteriorly displaced tibial condyles, and probably higher crural index, and heavy bodies (Arsuaga et al., 2015; Carretero et al., 2018), such as those living in a warm epoch similar to the present time in mean temperature (Blain et al., 2009), have a locomotion energy cost that is not as high as that of Neanderthals (due to the high crural index and the absolute length of the leg) but is higher than that of modern humans (due to their body size, Arsuaga et al., 2014; Carretero et al., 2018). Proper association of leg bones is needed to confirm these findings.

### 4.3 | Tibia biomechanical properties and activity

The tibiae of SH, as well as those of the femora (Rodríguez et al., 2018), exhibit thick cortices, high robusticity, and amygdaloid cross-sectional morphology similar to those of Neanderthals (Rodríguez et al., 2018). While thick cortices and high robusticity are primitive traits shared by all *Homo* species (Shang & Trinkaus, 2010; Trinkaus, 2009), the amygdaloid shape is not. The SH elliptical diaphysis shape may be an apomorphic trait that appeared in SH and was passed down to Neanderthals, as opposed to the more primitive, triangular diaphyseal shape observed in Boxgrove and Broken Hill (Lockey et al., 2022). The rounder shaft of SH tibiae implies greater variability in directional forces and suggests a high mobility pattern that likely involved not only walking or running but also frequent changes of direction (Shaw & Stock, 2009), indicating that SH individuals had an active lifestyle (Rodríguez et al., 2018) in agreement with findings for TD10 in Rodríguez-Hidalgo et al. (2015, 2016).

### 4.4 | Fibulae: Biomechanical interpretation

It has been shown that fibular robustness (relative to the tibia) corresponds with variation in inferred locomotor patterns among living hominoids (Hagihara & Nara, 2016; Marchi, 2007). Marchi and Shaw (2011) and Sparacello et al. (2014) concluded that this ratio is the consequence of fibula loading due to ankle movements, which are correlated with terrain properties and/or loading patterns of the leg (AP vs. ML movements). Unfortunately, we still do not have bone association. However, as previously stated, SH individuals likely had an active lifestyle that involved running and walking with frequent changes of direction, possibly during hunting activities detailed by Rodríguez-Hidalgo et al. (2015) and (2016) and depending on the topography of the terrain (Rodríguez et al., 2018).

The presence of a distal tibiofibular facet on a fossil fibula is difficult to interpret (Marchi, 2015). In any case, among the SH fibular specimens, the percentage of its presence in SH is around 25% while in modern humans is around 37.68%.

The SH specimens show a long STS but shorter than modern humans, although there are no statistical differences in maximum length, being Fib-IV, the shorter STS compared to the other specimens. Thus, SH specimens with lower STS distance may imply that SH has a longer belly and a shorter peroneal muscle than modern

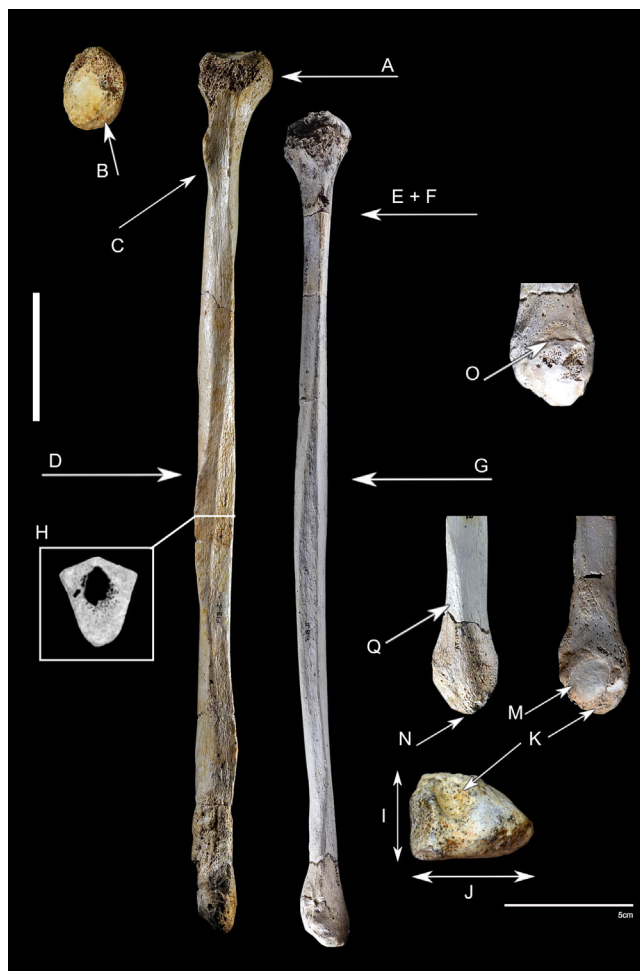


**FIGURE 21** SH main fibular traits. (a) large proximal epiphysis, (b) small styloid process, (c) variable development of muscular crests, (d) high diaphyseal robusticity, (e) high neck robusticity diaphysis, (f) minimum proximal perimeter located distally, (g) straight diaphysis, (h) thick cortices, (i) flatter mediolaterally distal epiphysis, (j) bigger anteroposterior diameter (k) and (l) short malleolar fossa, (m) elliptical-shaped and antero-superiorly sloped distal articular surface, (n) little development of the lateral malleolus, (p) short subcutaneous triangular surface (STS), (o) distal tibiofibular articular facet is variable.

humans. These muscles are active during the support and second half of the stance phase of locomotion in humans (Marchi, 2015). Thus, this shorter tendon in SH specimens can be related to a lower speed and a lower efficiency in the movement of the distal part of the limb than in modern humans.

Due to the small lateral malleolus in SH, the malleolar fossa is also smaller than in modern humans but similar to that of Shanidar Neanderthals. The malleolar fossa is the lateral insertion point for the posterior tibiofibular and posterior talofibular ligaments (Ebraheim et al., 2006), which, along with the anterior talofibular, calcaneofibular, and deltoid ligaments,

**TABLE 9** Basic statistics for adult fibulae of Sima de los Huesos (SH), Neanderthals, and Modern humans, including normality and Kruskal Wallis test with post hoc Mann–Whitney U when necessary.

	Valid	Mean	SD	Normality		Kruskall–Wallis		Posthoc: U-Mann Whitney		
				SW	p-value	KW	p-value	SH- <i>Homo sapiens</i>	SH-Neanderthals	Neanderthals- <i>H. sapiens</i>
Maximum length (M1)	<i>H. sapiens</i>	366.50	32.08	1.00	0.341	11.27	< 0.01	0.213	0.427	< 0.01
	Sima de los Huesos	346.67	14.57	0.86	0.263					
	Neanderthals	318.67	27.73	0.92	0.473					
Proximal Epiphysis Mediolateral diameter (M.4.1)	<i>H. sapiens</i>	21.65	3.01	0.99	0.142	4.48	0.106			
	Sima de los Huesos	24.92	2.13							
	Neanderthals	25.90								
Maximum Proximal diameter (T)	<i>H. sapiens</i>	12.73	1.95	0.99	0.048	4.43	0.109			
	Sima de los Huesos	16.18	1.61							
	Neanderthals	12.67	2.30	1.00	0.952					
Minimum Proximal diameter (T)	<i>H. sapiens</i>	10.37	1.78	0.97	< 0.01	1.52	0.427			
	Sima de los Huesos	11.64	1.49							
	Neanderthals	10.03	0.96	0.98	0.712					
Mediolateral diameter at midshaft (M3.1)	<i>H. sapiens</i>	13.80	2.47	0.99	< 0.01	1.24	0.539			
	Sima de los Huesos	14.04	1.47	0.90	0.385					
	Neanderthals	15.17	1.54	0.83	0.187					
Anteroposterior diameter at midshaft (M3.2)	<i>H. sapiens</i>	13.63	1.95	0.97	< 0.01	1.57	0.455			
	Sima de los Huesos	14.55	2.06	0.79	0.063					
	Neanderthals	21.86	12.59	0.85	0.181					
Distal epiphyseal breadth (T)	<i>H. sapiens</i>	21.57	3.04	0.99	0.739	7.20	0.027	0.025	0.854	0.775
	Sima de los Huesos	18.70	1.60	0.94	0.682					
	Neanderthals	18.93	2.70	0.97	0.65					

TABLE 9 (Continued)

									Kruskal- Wallis	Posthoc: U-Mann Whitney
Distal depth (T)	<i>H. sapiens</i>	181	25.63	2.99	0.98	0.03	3.81	0.149		
	Sima de los Huesos	6	27.95	2.58	0.96	0.795				
	Neanderthals	3	26.00	2.65	0.89	0.363				
Articular distal depth (T)	<i>H. sapiens</i>	181	20.42	2.55	0.98	0.04	3.09	0.213		
	Sima de los Huesos	6	20.47	3.51	0.78	0.04				
	Neanderthals	1	26.30							
Articular distal height (T)	<i>H. sapiens</i>	182	20.49	3.22	0.98	< 0.01	7.13	0.028	0.046	
	Sima de los Huesos	6	23.85	1.09	0.84	0.131				
	Neanderthals	1	20.10							
Minimum Proximal perimeter (M4a)	<i>H. sapiens</i>	176	39.99	33.97	0.13	< 0.01	2.76	0.251		
	Sima de los Huesos	2	45.00	7.07						
	Neanderthals	3	38.17	6.17	0.95	0.549				
Minimum perimeter at midshaft (M-4)	<i>H. sapiens</i>	180	42.49	5.18	0.98	< 0.01	2.35	0.309		
	Sima de los Huesos	5	45.00	3.39	0.67	< 0.01				
	Neanderthals	7	42.79	8.47	0.95	0.748				
STS length	<i>H. sapiens</i>	25	81.13	11.12	0.95	0.30	137.00	< 0.01 <sup>a</sup>		
	Sima de los Huesos	6	65.21	6.76	0.95	0.71				
	Neanderthals	0								

<sup>a</sup>Mann-Whitney U test was performed for two samples, due to not having values for neanderthals.

TABLE 10 Polarity of fibular traits.

Trait	Non-hominin apes	<i>A. afarensis</i>	<i>A. sediba</i>	Early <i>homo</i>	<i>H. erectus</i> s.l.	<i>H. naledi</i>	SH	<i>Neanderthals</i>	<i>H. sapiens</i>
Neck	Robust	Robust		Robust	Slender	Robust	Thick	Thick	Slender
Styloid process	No present					Well developed	Weak	Weak	Well developed
Shape of fibular head from a proximal view	Flat						Globous	Globous	Globous
Robusticity	Very Robust	Robust	Robust	Robust	Gracile	Robust	Robust	Robust	Gracile
Curvature	Anteriorly convex	Straight		Straight	Anteriorly convex	Straight	Straight	Straight	Straight or anteriorly concave
Articular facet orientation	Inferomedial	Inferomedial and distally				Medial	Distal and anterior	Distal and anterior	Medial
Malleolus	Projects laterally					Vertical	Posteriorly	Posteriorly	Vertical
Ridge between subcutaneous and peroneal	Sharp ridge	Sharp ridge	Sharp ridge	Sharp ridge		Sharp ridge	Gentle arch	Gentle arch	Gentle arch
Proximal border of articular facet	Oblique	Oblique		Oblique		Oblique	Oblique	Oblique	Horizontal
Relationship between fibular and tibial malleoli	Long								Short
Axis between the two malleoli relative to ground surface	Not parallel								Parallel

Shading boxes mean: Without data.

control and limit the mobility of the ankle joint (Kleipool & Blankevoort, 2010). Marchi et al. (2022) suggest that the deeper and wider malleolar fossa in great apes compared to humans might be the consequence of a larger talofibular ligament in the former, which is possibly due to the higher frequency and magnitude of dorsiflexion experienced during climbing behavior by great apes. Thus, SH specimens with a smaller malleolar fossa than modern humans may have experienced less magnitude of dorsiflexion than modern humans but similar to that of Neanderthals shown in the figures of Shanidar Neandertals (Trinkaus, 1983).

## 5 | CONCLUSIONS

The tibiae and fibulae remains from SH resemble those of Neanderthals more than other middle Pleistocene individuals. The tibiae have pleiomorphic characteristics, including posteriorly displaced tibial condyles, robust and curved shape, and a platymeric diaphysis and amygdaloid cross-section shape, which they share with Neanderthals. However, the tibiae are longer than those of Neanderthals, which may be related to a higher crural index similar to that of modern humans, resulting in better locomotor efficiency than Neanderthals. The fibulae are also similar to those of Neanderthals in having higher robusticity in both epiphysis and the diaphysis, and a small malleolar fossa.

### AUTHOR CONTRIBUTIONS

**Laura Rodríguez:** Conceptualization; investigation; writing – original draft; methodology; writing – review and editing; visualization; formal analysis. **Rebeca García-González:** Conceptualization; investigation; methodology; visualization; writing – review and editing; formal analysis. **Juan Luis Arsuaga:** Funding acquisition; writing – review and editing; visualization; project administration; supervision. **José-Miguel Carretero:** Conceptualization; investigation; funding acquisition; writing – review and editing; data curation; project administration; supervision.

### ACKNOWLEDGMENTS

We have benefitted from fruitful discussions with our colleagues from the Centro UCM-ISCIH sobre Evolución y Comportamiento Humanos of Madrid and the Laboratorio de Evolución Humana at the University of Burgos. Thanks to the anonymous reviewers of the manuscript for their valuable comments. We thank our companions in the Atapuerca research and SH excavation team for their invaluable

dedication to the ongoing work at the SH site. Thanks to Maria Cruz Ortega for her extraordinary and patient restoration of the fossils. Our acknowledgment and gratitude to Javier Trueba for the extraordinary graphic documentation of the SH fossils and fieldwork under very demanding conditions. The following individuals and their institutions for access to the modern and fossil comparative materials: P. Mennecier and A. Froment (Muséum National d'Histoire Naturelle); Y. Haile-Selassie, B. Latimer, and L. Jellema (Cleveland useum of Natural History); E. Cunha and A. L. Santos (Coimbra University) and A. Marcal (Bocage Museum) and T. Holliday (Tulane University). The fossil analyzed in this work are from the “Colección Museística de Castilla y León” of the Junta de Castilla y León.

### FUNDING INFORMATION

Grant PID2021-122355NB-C31 funded by MCIN/AEI/10.13039/501100011033 and “ERDF A way of making Europe”, Fieldwork at the Atapuerca sites is funded by the Junta de Castilla y León and the Fundación Atapuerca.

### CONFLICT OF INTEREST STATEMENT

The authors declare no conflicts of interest.

### ORCID

Laura Rodríguez  <https://orcid.org/0000-0002-5090-1582>

Rebeca García-González  <https://orcid.org/0000-0002-1035-6655>

José-Miguel Carretero  <https://orcid.org/0000-0003-0409-8087>

### REFERENCES

- Acsadi, G., & Nemeskeri, J. (1970). *History of human life span and mortality*. Akademiai Kiadó Publishers.
- Aiello, L. C., & Dean, C. (1990). *An introduction to human evolutionary anatomy*. Academic Press Limited.
- Aiello, L. C., & Wheeler, P. (2003). Neanderthal thermoregulation and the glacial climate. In T. H. van Andel & W. Davies (Eds.), *Neanderthals and modern humans in the European landscape during the last glaciation*. McDonald Institute for Archaeological Research.
- Allen, J. A. (1877). The influence of physical conditions in the genesis of species. *Radical Review*, 1, 108–140.
- Antón, S. C. (2003). Natural history of *Homo erectus*. *American Journal of Physical Anthropology*, 122(S37), 126–170. <https://doi.org/10.1002/ajpa.10399>
- Arsuaga, J. L., Bermudez, J. M., & Carbonell, E. (1997). The Sima de los Huesos Hominid Site. *Journal of Human Evolution*, 33, 105–421.
- Arsuaga, J. L., Carretero, J.-M., Lorenzo, C., Gómez-Olivencia, A., Pablos, A., Rodríguez, L., García-González, R., Bonmatí, A., Quam, R. M., Pantoja-Pérez, A., Martínez, I., Aranburu, A.,

- Gracia-Téllez, A., Poza-Rey, E., Sala, N., García, N., Alcázar de Velasco, A., Cuenca-Bescós, G., Bermúdez de Castro, J. M., & Carbonell, E. (2015). Postcranial morphology of the middle Pleistocene humans from Sima de los Huesos, Spain. *Proceedings of the National Academy of Sciences of the United States of America*, 112(37), 11524–11529. <https://doi.org/10.1073/pnas.1514828112>
- Arsuaga, J.-L., Lorenzo, C., Carretero, J.-M., Gracia, A., Martínez, I., García, N., de Castro, J.-M. B., & Carbonell, E. (1999). A complete human pelvis from the middle Pleistocene of Spain. *Nature*, 399(6733), 255–258. <https://doi.org/10.1038/20430>
- Arsuaga, J. L., Martínez, I., Arnold, L. J., Aranburu, A., Gracia-Tellez, A., Sharp, W. D., Quam, R., Falgueres, C., Pantoja-Perez, A., Bischoff, J., Poza-Rey, E., Parés, J. M., Carretero, J. M., Demuro, M., Lorenzo, C., Sala, N., Martínón-Torres, M., García, N., Alcazar de Velasco, A., ... Carbonell, E. (2014). Neandertal roots: Cranial and chronological evidence from Sima de los Huesos. *Science*, 344, 1358–1363.
- Auerbach, B. M., & Sylvester, A. D. (2011). Allometry and apparent paradoxes in human limb proportions: Implications for scaling factors. *American Journal of Physical Anthropology*, 144, 382–391.
- Autodesk, I. (2012). Autocad. [Software]. [www.autodesk.es](http://www.autodesk.es).
- Barnett, C. H., & Napier, J. R. (1953). The rotatory mobility of the fibula in eutherian mammals. *Journal of Anatomy*, 87(1), 11–21.
- Biewener, A. A. (2016). Locomotion as an emergent property of muscle contractile dynamics. *Journal of Experimental Biology*, 219(2), 285–294. <https://doi.org/10.1242/jeb.123935>
- Blackburn, T. M., Gaston, K. J., & Loder, N. (1999). Geographic gradients in body size: A clarification of Bergmann's rule. *Diversity and Distributions*, 5(4), 165–174. <https://doi.org/10.1046/j.1472-4642.1999.00046.x>
- Blain, H.-A., Bailon, S., Cuenca-Bescós, G., Arsuaga, J. L., Bermúdez de Castro, J. M., & Carbonell, E. (2009). Long-term climate record inferred from early-middle Pleistocene amphibian and squamate reptile assemblages at the Gran Dolina cave, Atapuerca, Spain. *Journal of Human Evolution*, 56(1), 55–65. <https://doi.org/10.1016/j.jhevol.2008.08.020>
- Bogin, B., & Ríos, L. (2003). Rapid morphological change in living humans: Implications for modern human origins. *Comparative Biochemistry and Physiology Part A*, 136, 71–84.
- Bogin, B., Smith, P., Orden, A. B., Varela Silva, M. I., & Loucky, J. (2002). Rapid change in height and body proportions of Maya American children. *American Journal of Human Biology*, 14(6), 753–761. <https://doi.org/10.1002/ajhb.10092>
- Bonmatí, A., Gómez-Olivencia, A., Arsuaga, J. L., Carretero, J. M., Gracia, A., Martínez, I., Lorenzo, C., Bermúdez de Castro, J. M., & Carbonell, E. (2010). Middle Pleistocene lower back and pelvis from an aged human individual from the Sima de los Huesos site, Spain. *Proceedings of the National Academy of Sciences of the United States of America*, 107(43), 18386–18391.
- Boule, M. (1911). L'Homme Fossile de La Chapelle aux Saints. *Annales de Paléontologie* Masson et C, Editeurs, Paris.
- Buikstra, J., & Ubelaker, D. H. (1994). Standards for data collection from human skeletal remains.
- Cardoso, H. F. (2006). Brief communication: The collection of identified human skeletons housed at the Bocage museum (National Museum of Natural History), Lisbon, Portugal. *American Journal of Physical Anthropology*, 129(2), 173–176.
- Carretero, J.-M., García-González, R., Rodríguez, L., & Arsuaga, J.-L. (2024a). Main anatomical characteristics of the hominin fossil humeri from the Sima de los Huesos Middle Pleistocene site, Sierra de Atapuerca, Burgos, Spain: An update. *Anatomical Record*, 307(7), 2519–2549. <https://doi.org/10.1002/ar.25194>
- Carretero, J.-M., Rodríguez, L., García-González, R., & Arsuaga, J.-L. (2024b). Main morphological characteristics and sexual dimorphism of the hominin adult femora from Sima de los Huesos Middle Pleistocene site (Sierra de Atapuerca, Spain). *Anatomical Record*, 307(7), 2575–2605.
- Carretero, J. M., Haile-Selassie, Y., Rodríguez, L., & Arsuaga, J. L. (2009). A partial distal humerus from the middle Pleistocene deposits at Bodo, middle awash, Ethiopia. *Anthropological Science*, 117, 19–31.
- Carretero, J.-M., Rodríguez, L., García-González, R., Arsuaga, J.-L., Gómez-Olivencia, A., Lorenzo, C., Bonmatí, A., Gracia, A., Martínez, I., & Quam, R. (2012). Stature estimation from complete long bones in the middle Pleistocene humans from the Sima de los Huesos, sierra de Atapuerca (Spain). *Journal of Human Evolution*, 62(2), 242–255. <https://doi.org/10.1016/j.jhevol.2011.11.004>
- Carretero, J. M., Rodriguez, L., García-González, R., Quam, R., & Arsuaga, J. L. (2018). Exploring bone volume and skeletal weight in the middle Pleistocene humans from the Sima de los Huesos site (sierra de Atapuerca, Spain). *Journal of Anatomy*, 233, 740–754. <https://doi.org/10.1111/joa.12886>
- Churchill, S. E. (1998). Cold adaptation, heterochrony and Neandertals. *Evolutionary Anthropology*, 7, 46–60.
- Churchill, S. E. (2006). Bioenergetic perspectives on Neanderthal thermoregulatory and activity budgets. In J. J. Hublin, K. Harvati, & T. Harrison (Eds.), *Neanderthals revisited: New approaches and perspectives* (pp. 113–134). Springer.
- Coqueugniot, H., & Weaver, T. D. (2007). Brief communication: Infracranial maturation in the skeletal collection from Coimbra, Portugal: New aging standards for epiphyseal union. *American Journal of Physical Anthropology*, 134(3), 424–437.
- Ebraheim, N. A., Taser, F., Shafiq, Q., & Yeasting, R. A. (2006). Anatomical evaluation and clinical importance of the tibiofibular syndesmosis ligaments. *Surgical and Radiologic Anatomy*, 28, 142–149. <https://doi.org/10.1007/s00276-006-0077-0>
- Frelat, M. A., & Mitteroecker, P. (2011). Postnatal ontogeny of tibia and femur form in two human populations: A multivariate morphometric analysis. *American Journal of Human Biology*, 23(6), 796–804. <https://doi.org/10.1002/ajhb.21217>
- Froehle, A. W., & Churchill, S. E. (2009). Energetic competition between neandertals and anatomically modern humans. *Paleo-Anthropology*, 2009, 96–116.
- García-González, R., Rodríguez, L., Salazar-Fernández, A., Arsuaga, J. L., & Carretero, J.-M. (2024). Updated study of adult and subadult pectoral girdle bones from Sima de los Huesos site (Sierra de Atapuerca, Burgos, Spain). Anatomical and age estimation keys. *Anatomical Record*, 307(7), 2491–2518. <https://doi.org/10.1002/ar.25158>
- Gilbert, W. H. (2008). Daka member hominid postcranial remains. In W. H. Gilbert & B. Asfaw (Eds.), *Homo erectus, Pleistocene evidence from middle awash, Ethiopia* (pp. 373–396). University of California Press.

- Grine, F. E., Jungers, W. L., Tobias, P. V., & Pearson, O. M. (1995). Fossil Homo femur from berg Aukas Northern Namibia. *American Journal of Biological Anthropology*, 97, 151–185.
- Hagihara, Y., & Nara, T. (2016). Morphological features of the fibula in Jomon hunter-gatherers from the shell mounds of the Pacific coastal area. *American Journal of Physical Anthropology*, 160(4), 708–718. <https://doi.org/10.1002/ajpa.23000>
- Heim, J. L. (1982). *Les Hommes fossiles de la Ferrassie: Vol. Tome II: Squelette des membres*. Masson.
- Hicks, J., Arnold, A., Anderson, F., Schwartz, M., & Delp, S. (2007). The effect of excessive tibial torsion on the capacity of muscles to extend the hip and knee during single-limb stance. *Gait and Posture*, 26, 546–552.
- Higgins, R. W., & Ruff, C. B. (2011). The effects of distal limb segment shortening on locomotor efficiency in sloped terrain: Implications for Neandertal locomotor behavior. *American Journal of Physical Anthropology*, 146(3), 336–345. <https://doi.org/10.1002/ajpa.21575>
- Holliday, T. W. (1997). Body proportions in late Pleistocene Europe and modern human origins. *Journal of Human Evolution*, 32, 423–447.
- Holliday, T. W. (1999). Brachial and crural indices of European late upper Paleolithic and Mesolithic humans. *Journal of Human Evolution*, 36, 549–566.
- Holliday, T. W., & Falsetti, A. (1995). Lower limb length of European early modern humans in relation to mobility and climate. *Journal of Human Evolution*, 29, 141–153.
- Huguet, R., Saladié, P., Cáceres, I., Díez, C., Rosell, J., Bennàsar, M., Blasco, R., Esteban-Nadal, M., Gabucio, M. J., Rodríguez-Hidalgo, A., & Carbonell, E. (2013). Successful subsistence strategies of the first humans in south-western Europe. *Quaternary International*, 295, 168–182. <https://doi.org/10.1016/j.quaint.2012.11.015>
- Jakob, R. P., Haertel, M., & Stussi, E. (1980). Tibial torsion calculated by computerised tomography. *The Journal of Bone and Joint Surgery*, 62-B(2), 238–242.
- Jantz, R. J., & Moore-Jansen, P. H. (2000). *Database for forensic anthropology in the United States, 1962–1991*. Inter-university Consortium for Political and Social Research.
- Kleipool, R. P., & Blankevoort, L. (2010). The relation between geometry and function of the ankle joint complex: A biomechanical review. *Knee Surgery, Sports Traumatology, Arthroscopy*, 18(5), 618–627. <https://doi.org/10.1007/s00167-010-1088-2>
- Kramer, P. A., & Eck, G. G. (2000). Locomotor energetics and leg length in hominid bipedality. *Journal of Human Evolution*, 38, 651–666.
- Kramer, P. A., & Silvestre, A. (2009). Bipedal form and locomotor function: Understanding the effects of size and shape on velocity and energetics. *PaleoAnthropology*, 2009, 238–251.
- Lockey, A. L., Rodríguez, L., Martín-Francés, L., Arsuaga, J. L., Bermúdez de Castro, J. M., Crété, L., Martínón-Torres, M., Parfitt, S., Pope, M., & Stringer, C. (2022). Comparing the Boxgrove and Atapuerca (Sima de los Huesos) human fossils: Do they represent distinct paleodemes? *Journal of Human Evolution*, 172, 103253. <https://doi.org/10.1016/j.jhevol.2022.103253>
- Marchi, D. (2007). Relative strength of the tibia and fibula and locomotor behavior in hominoids. *Journal of Human Evolution*, 53(6), 647–655. <https://doi.org/10.1016/j.jhevol.2007.05.007>
- Marchi, D. (2015). Using the morphology of the hominoid distal fibula to interpret arboreality in Australopithecus afarensis. *Journal of Human Evolution*, 85, 136–148. <https://doi.org/10.1016/j.jhevol.2015.06.002>
- Marchi, D., Rimoldi, A., García-Martínez, D., & Bastir, M. (2022). Morphological correlates of distal fibular morphology with locomotion in great apes, humans, and Australopithecus afarensis. *American Journal of Biological Anthropology*, 178(2), 286–300. <https://doi.org/10.1002/ajpa.24507>
- Marchi, D., & Shaw, C. N. (2011). Variation in fibular robusticity reflects variation in mobility patterns. *Journal of Human Evolution*, 61(5), 609–616. <https://doi.org/10.1016/j.jhevol.2011.08.005>
- Marchi, D., Walker, C. S., Wei, P., Holliday, T. W., Churchill, S. E., Berger, L. R., & DeSilva, J. M. (2017). The thigh and leg of *Homo naledi*. *Journal of Human Evolution*, 104, 174–204. <https://doi.org/10.1016/j.jhevol.2016.09.005>
- Martin, R., & Saller, K. (1957). *Lehrbuch der Anthropologie.: Vol. Band 1*. Gustav Fischer Verlag.
- Meulam, J. J., & Heiser, W. J. (2019). IBM SPSS Categories 26.
- Mizushima, S., Suwa, G., & Hirata, K. (2016). A comparative analysis of fetal to subadult femoral midshaft bone distribution of prehistoric Jomon hunter-gatherers and modern Japanese. *Anthropological Science*, 124(1), 1–15. <https://doi.org/10.1537/ase.151104>
- Ogden, J. A. (1974). The anatomy and function of the proximal tibiofibular joint. *Clinical Orthopaedics and Related Research* (1976–2007), 101, 186–191. [https://journals.lww.com/corr/Fulltext/1974/06000/The\\_Anatomy\\_and\\_Function\\_of\\_the\\_Proximal.28.aspx](https://journals.lww.com/corr/Fulltext/1974/06000/The_Anatomy_and_Function_of_the_Proximal.28.aspx)
- Olivier, G. (1969). *Practical anthropology* (M. A. MacConail, Trad.). Charles C. Thomas.
- Payne, R. C., Crompton, R. H., Isler, K., Savage, R., Vereecke, E. E., Günther, M. M., Thorpe, S. K. S., & D'Aouit, K. (2006). Morphological analysis of the hindlimb in apes and humans. I. Muscle Architecture. *Journal of Anatomy*, 208(6), 709–724. <https://doi.org/10.1111/j.1469-7580.2005.00433.x-ii>
- Phenice, T. W. (1969). A newly developed visual method of sexing the os pubis. *American Journal of Physical Anthropology*, 30, 297–301.
- Richards, M. P., Pettitt, P. B., Trinkaus, E., Smith, F. H., Paunović, M., & Karavanić, I. (2000). Neanderthal diet at Vindija and Neanderthal predation: The evidence from stable isotopes. *Proceedings of the National Academy of Sciences of the United States of America*, 97(13), 7663–7666. <https://doi.org/10.1073/pnas.120178997>
- Roberts, M. B., Stringer, C. B., & Parfitt, S. A. (1994). A hominid tibia from middle Pleistocene sediments at Boxgrove, UK. *Nature*, 369(6478), 311–313. <https://doi.org/10.1038/369311a0>
- Rodríguez, L., Carretero, J. M., García-González, R., & Arsuaga, J. L. (2018). Cross-sectional properties of the lower limb long bones in the middle Pleistocene Sima de los Huesos sample (Sierra de Atapuerca, Spain). *Journal of Human Evolution*, 117, 1–12. <https://doi.org/10.1016/j.jhevol.2017.11.007>
- Rodríguez, L., García-González, R., Arsuaga, J. L., & Carretero, J.-M. (2024). Uncovering the adult morphology of the forearm bones from the Sima de los Huesos site in Atapuerca (Spain), with comments on biomechanical features. *The Anatomical Record*, 307(7), 2550–2574. <https://doi.org/10.1002/ar.25281>

- Rodríguez-Hidalgo, A., Rivals, F., Saladié, P., & Carbonell, E. (2016). Season of bison mortality in TD10.2 bone bed at Gran Dolina site (Atapuerca): Integrating tooth eruption, wear, and microwear methods. *Journal of Archaeological Science: Reports*, 6, 780–789. <https://doi.org/10.1016/j.jasrep.2015.11.033>
- Rodríguez-Hidalgo, A., Saladié, P., Ollé, A., & Carbonell, E. (2015). Hominin subsistence and site function of TD10.1 bone bed level at Gran Dolina site (Atapuerca) during the late Acheulean. *Journal of Quaternary Science*, 30, 679–701. <https://doi.org/10.1002/jqs.2815>
- Rosenberg, K. R., Zúñe, L., & Ruff, C. B. (2006). Body size, body proportions and encephalization in a middle Pleistocene archaic human from northern China. *Proceedings of the National Academy of Sciences of the United States of America*, 103(10), 3552–3556.
- Ruff, C. B. (2005). Mechanical determinants of bone form: Insights from skeletal remains. *Journal of Musculoskeletal & Neuronal Interactions*, 5(3), 202–212.
- Ruff, C. B., & Hayes, W. C. (1983). Cross-sectional geometry of pecos pueblo femora and tibiae—a biomechanical investigation: I. Method and general patterns of variation. *American Journal of Physical Anthropology*, 60, 359–381.
- Ruff, C. B., & Hayes, W. C. (1988). Sex differences in age-related remodeling of femur and tibia. *Journal of Orthopaedic Research*, 6, 886–896.
- Ruff, C. B., Holt, B. M., & Trinkaus, E. (2006). Who's afraid of the big bad Wolff?: «Wolff's law» and bone functional adaptation. *American Journal of Biological Anthropology*, 129, 484–498.
- Ruff, C. B., Trinkaus, E., Walker, A., & Spencer-Larsen, C. (1993). Postcranial robusticity in Homo I: Temporal trends and mechanical interpretation. *American Journal of Physical Anthropology*, 91, 21–53.
- Saladié, P., Rodríguez-Hidalgo, A., Marín, J., Vallverdú i Poch, J., & Carbonell, E. (2018). The top of the Gran Dolina (Atapuerca, Spain) sequence: A zooarchaeological and occupational perspective. *Quaternary Science Reviews*, 195, 48–71. <https://doi.org/10.1016/j.quascirev.2018.07.010>
- Schwartz, H. S., & Lakin, G. (2003). The effect of tibial torsion on the dynamic function of the soleus during gait. *Gait and Posture*, 17, 113–118.
- Shang, H., & Trinkaus, E. (2010). *The early modern human from Tianyuan cave, China*. Texas A&M University Press.
- Shaw, C. N., & Stock, J. T. (2009). Intensity, repetitiveness, and directionality of habitual adolescent mobility patterns influence the tibial diaphysis morphology of athletes. *American Journal of Physical Anthropology*, 140, 149–159.
- Simpson, S. W., Quade, J., Levin, N. E., Butler, R., Dupont-Nivet, G., Everett, M., & Semaw, S. (2008). A female *Homo erectus* pelvis from Gona, Ethiopia. *Science*, 322, 1089–1092.
- Sparacello, V. S., Marchi, D., & Shaw, C. N. (2014). The importance of considering fibular robusticity when inferring the mobility patterns of past populations. In K. J. Carlson & D. Marchi (Eds.), *Reconstructing mobility* (pp. 91–110). Springer.
- Squyres, N., & Ruff, C. B. (2015). Body mass estimation from knee breadth, with application to early hominins. *American Journal of Physical Anthropology*, 158(2), 198–208. <https://doi.org/10.1002/ajpa.22789>
- Studel-Numbers, K. L., & Tilkens, M. J. (2004). The effect of lower limb length on the energetic cost of locomotion: Implications for fossil hominins. *Journal of Human Evolution*, 47(1), 95–109.
- Stringer, C., Trinkaus, E., Roberts, M. B., Parfitt, S. A., & Macphail, R. I. (1998). The middle Pleistocene human tibia from Boxgrove. *Journal of Human Evolution*, 34, 509–547.
- Terradillos-Bernal, M., & Rodríguez-Álvarez, X.-P. (2014). The influence of raw material qualities in the lithic technology of Gran Dolina (Units TD6 and TD10) and Galería (Sierra de Atapuerca, Burgos, Spain): A view from experimental archeology. *Comptes Rendus Palevol*, 13, 527–542. <https://doi.org/10.1016/j.crv.2014.02.002>
- Trinkaus, E. (1975). Squatting among the neandertals: A problem in the behavioral interpretation of skeletal morphology. *Journal of Archaeological Science*, 2(4), 327–351. [https://doi.org/10.1016/0305-4403\(75\)90005-9](https://doi.org/10.1016/0305-4403(75)90005-9)
- Trinkaus, E. (1981). Neanderthal limb proportions and cold adaptation. In C. Stringer (Ed.), *Aspects of human evolution*. Taylor and Francis.
- Trinkaus, E. (1983). *The Shanidar Neandertals*. Academic Press.
- Trinkaus, E. (1993). Femoral neck-shaft angles of the Qafzeh-Skhul early modern humans, and activity levels among immature near eastern middle Paleolithic hominids. *Journal of Human Evolution*, 25, 393–416.
- Trinkaus, E. (2009). The human tibia from Broken Hill, Kabwe, Zambia. *PaleoAnthropology*, 2009, 145–165.
- Trinkaus, E., & Rhoads, M. L. (1999). Neandertal knees: Power lifters in the Pleistocene? *Journal of Human Evolution*, 37(6), 833–859.
- Trinkaus, E., & Ruff, C. B. (2012). Femoral and tibial diaphyseal cross-sectional geometry in pleistocene Homo. *PaleoAnthropology*, 2012, 13–62.
- Trinkaus, E., Maley, B., & Buzhilova, A. P. (2008). Brief Communication: Paleopathology of the Kiik-Koba 1 Neandertal. *American Journal of Physical Anthropology*, 137, 106–112.
- Trinkaus, E., Ruff, C. B., & Conroy, G. C. (1999). The anomalous archaic Homo femur from berg Aukas, Namibia. A biomechanical assessment. *American Journal of Physical Anthropology*, 110, 379–391.
- Villa, P., & D'errico, F. (2001). Bone and ivory points in the lower and middle Paleolithic of Europe. *Journal of Human Evolution*, 41(2), 69–112.
- Ward, C. V. (2002). Interpreting the posture and locomotion of Australopithecus afarensis: Where do we stand? *American Journal of Physical Anthropology*, 119, 185–215. <https://doi.org/10.1002/ajpa.10185>
- Weaver, T. D. (2009). The meaning of Neandertal skeletal morphology. *Proceedings of the National Academy of Sciences of the United States of America*, 106, 16028–16033.
- White, T. D., Black, M. T., & Folkens, P. A. (Eds.). (2012). *Human Osteology*. Academic Press.

**How to cite this article:** Rodríguez, L., García-González, R., Arsuaga, J. L., & Carretero, J.-M. (2024). Exploring the morphology of adult tibia and fibula from Sima de los Huesos site in sierra de Atapuerca, Burgos, Spain. *The Anatomical Record*, 307(7), 2606–2634. <https://doi.org/10.1002/ar.25336>